Novel functional interaction between the plasma membrane Ca2+ pump 4b and the proapoptotic tumor suppressor Ras-associated factor 1 (RASSF1).

THE JOURNAL OF BIOLOGICAL CHEMISTRY Vol. 279, No. 30, Issue of July 23, pp. 31318–31328, 2004
Printed in U.S.A.

Novel Functional Interaction between the Plasma Membrane Ca^{2+} Pump 4b and the Proapoptotic Tumor Suppressor Ras-associated Factor 1 (RASSF1)*

Received for publication, July 14, 2003, and in revised form, May 14, 2004
Published, JBC Papers in Press, May 15, 2004, DOI 10.1074/jbc.M307557200

Angel L. Armesilla‡§, Judith C. Williams‡§, Mamta H. Buch‡, Adam Pickard‡, Michael Emerson‡, Elizabeth J. Cartwright‡, Delvac Oceandy‡, Michele D. Vos¶, Sheona Gillies‡, Geoffrey J. Clark¶, and Ludwig Neyses‡‖

From the ‡Division of Cardiology, University of Manchester, Manchester M13 9PT, United Kingdom and the ¶Department of Cell and Cancer Biology, NCI, National Institutes of Health, Rockville, Maryland 20850-3300

Plasma membrane calmodulin-dependent calcium ATPases (PMCAs) are enzymatic systems implicated in the extrusion of calcium from the cell. We and others have previously identified molecular interactions between the cytoplasmic COOH-terminal end of PMCA and PDZ domain-containing proteins. These interactions suggested a new role for PMCA as a modulator of signal transduction pathways. The existence of other intracellular regions in the PMCA molecule prompted us to investigate the possible participation of other domains in interactions with different partner proteins. A two-hybrid screen of a human fetal heart cDNA library, using the region 652–840 of human PMCA4b (located in the catalytic, second intracellular loop) as bait, revealed a novel interaction between PMCA4b and the tumor suppressor RASSF1, a Ras effector protein involved in H-Ras-mediated apoptosis. Immunofluorescence co-localization, immunoprecipitation, and glutathione *S*-transferase pull-down experiments performed in mammalian cells provided further confirmation of the physical interaction between the two proteins. The interaction domain has been narrowed down to region 74–123 of RASSF1C (144–193 in RASSF1A) and 652–748 of human PMCA4b. The functionality of this interaction was demonstrated by the inhibition of the epidermal growth factor-dependent activation of the Erk pathway when PMCA4b and RASSF1 were co-expressed. This inhibition was abolished by blocking PMCA/RASSSF1 association with an excess of a green fluorescent protein fusion protein containing the region 50–123 of RASSF1C. This work describes a novel protein-protein interaction involving a domain of PMCA other than the COOH terminus. It suggests a function for PMCA4b as an organizer of macromolecular protein complexes, where PMCA4b could recruit diverse proteins through interaction with different domains. Furthermore, the functional association with RASSF1 indicates a role for PMCA4b in the modulation of Ras-mediated signaling.

Plasma membrane calmodulin-dependent calcium ATPases (PMCAs)[1] are enzymatic high affinity Ca^{2+}-extruding systems that are thought to play a key role in maintaining intracellular calcium homeostasis in nonexcitable cells (reviewed in Ref. 1).

PMCAs are P-type ATPases (2, 3), characterized by the formation of an aspartyl phosphate intermediate during the reaction cycle. At present, four different PMCA isoforms, PMCA1–4, have been identified in mammals as the products of four independent genes (4–10). PMCA1 and PMCA4 are ubiquitously expressed, whereas PMCA2 and PMCA3 show a more restricted cell- and tissue-specific pattern of expression (5, 10).

The primary protein structure of PMCAs comprises 10 membrane-spanning segments, two major cytosolic loops, and NH_2 and COOH cytoplasmic tails. The COOH-terminal tail contains an autoinhibitory domain (situated ~40 amino acids downstream of the last transmembrane domain) that binds Ca^{2+}-calmodulin and plays a major role in the regulation of the activity of the enzyme (11–13). In the absence of Ca^{2+}-calmodulin, this domain interacts with two different regions of PMCA located in the first and second intracellular loops (13, 14). This intramolecular interaction keeps the pump in an inactive state. Elevation in the Ca^{2+}-calmodulin levels prompts high affinity binding to the autoinhibitory domain, releasing inhibition, and stimulating pump activity.

Our group and others have identified other molecular interactions involving the COOH-terminal region and PDZ domain-containing proteins. These proteins include members of the membrane-associated guanylate kinase (MAGUK) family (15, 16), cytoskeletal proteins (17), Na^+/H^+ exchanger regulatory factor 2 (18), nitric-oxide synthase I (nNOS) (19), calcium/calmodulin-dependent serine protein kinase (CASK) (20), and a novel protein named PISP (PMCA-interacting single-PDZ protein) (21). These interactions suggest a new function of PMCA as a modulator of intracellular signaling pathways. In fact, by placing interaction partners in a cellular microenvironment, where the concentrations of Ca^{2+} and calmodulin are kept low, PMCA was shown to negatively modulate the activity of nNOS

* This work was supported by a Medical Research Council International Appointee Grant G0200020 (to L. N.) and a Wellcome Trust entry-level training fellowship (to M. H. B.). The costs of publication of this article were defrayed in part by the payment of page charges. This article must therefore be hereby marked "*advertisement*" in accordance with 18 U.S.C. Section 1734 solely to indicate this fact.

§ These authors contributed equally to this work.

‖ To whom correspondence should be addressed: Division of Cardiology, Rm. 1.302, Stopford Bldg., University of Manchester, Oxford Rd., Manchester M13 9PT, United Kingdom. Tel.: 44-161-276-5738; Fax: 44-161-276-8904; E-mail: ludwig.neyses@cmmc.nhs.uk.

[1] The abbreviations used are: PMCA, plasma membrane Ca^{2+}-ATPase; DMEM, Dulbecco's modified Eagle's medium; EGF, epidermal growth factor; Erk, extracellular signal-regulated protein kinase; FCS, fetal calf serum; hPMCA, human plasma membrane Ca^{2+}-ATPase; PBS, phosphate-buffered saline; PMSF, phenylmethanesulfonyl fluoride; X-gal, 5-bromo-4-chloro-3-indolyl-β-D-galactopyranoside; nNOS, nitric-oxide synthase I; MAGUK, membrane-associated guanylate kinase; GST, glutathione *S*-transferase; CASK, calcium/calmodulin-dependent serine protein kinase; FITC, fluorescein isothiocyanate; CARD, caspase recruitment domain; HEK, human embryonic kidney; RIPA, radioimmunoprecipitation assay; TBS, Tris-buffered saline; TBS-T, Tris-buffered saline plus Tween 20.

(19) and CASK (20). These interactions are dependent on the presence of the E(T/S)*X*(V/L)* sequence in the COOH-cytoplasmic end of PMCA, and PDZ domains in the partner proteins. However, the existence of other intracellular domains in the PMCA polypeptide chain, and the previous reports of a functional interaction between PMCA and calmodulin (a protein without PDZ domains), prompted us to investigate whether other regions are implicated in interactions with different partner proteins.

To test this hypothesis, we performed a two-hybrid screen of a human fetal heart cDNA library. We used the sequence from amino acids 652 to 840 (located in the catalytic, second intracellular loop, between transmembrane domains 4 and 5) of the human PMCA4b isoform (accession no. NM_001684) as bait.

A positive clone encoding a partial sequence of the tumor suppressor RASSF1, a Ras effector protein that mediates the apoptotic effects of H-Ras (22, 23), was isolated. We have further characterized RASSF1 as a novel interaction partner of PMCA. Interaction of PMCA with RASSF1 significantly inhibited the EGF-dependent activation of the mitogen-activated protein kinase Erk, indicating a role for PMCA as a modulator of EGF-mediated Ras signaling pathways via interaction with RASSF1.

This work shows a novel protein-protein interaction involving a domain of PMCA other than the COOH terminus. It suggests a role for PMCA as an organizer of macromolecular protein complexes, and a regulator of intracellular signaling pathways in the microenvironment of these multiprotein complexes.

EXPERIMENTAL PROCEDURES

Cell Culture, Isolation, and Culture of Neonatal Rat Cardiomyocytes—HEK 293 cells were maintained in Dulbecco's modified Eagle's medium (DMEM) (Invitrogen) supplemented with 10% FCS and 1% penicillin/streptomycin.

Isolation of neonatal rat cardiomyocytes was performed on hearts removed from 1–3-day-old rats. Hearts were cut in small pieces and ventricular tissue digested by several rounds of 10-min incubation in a filter-sterilized solution of collagenase A (0.3 mg/ml), pancreatin (0.6 mg/ml), ADS buffer, pH 7.35 (0.68% NaCl (w/v), 0.476% Hepes (w/v), 0.012% NaH_2PO_4 (w/v), 0.1% glucose (w/v), 0.04% KCl (w/v), 0.01% $MgSO_4$ (w/v)) at 37 °C with shaking. Each round of digestion was finished by addition of 2 ml of FCS. Digestions were pooled and cells collected by centrifugation at 700 rpm for 4 min. Cell pellet was resuspended in plating media (68% DMEM, 17% Medium 199, 10% horse serum, 5% FCS) (1 ml/pup), plated on 100 × 20-mm tissue culture dishes (Falcon), and incubated for 60 min at 37 °C, 5% CO_2 to remove cardiac fibroblasts. Supernatants containing cardiomyocytes were plated on 22 × 22-mm collagen-coated coverslips and further incubated overnight at 37 °C, 5% CO_2 to allow cellular attachment. The following day, cells were washed with PBS and plating media were replaced with maintenance media (79.5% DMEM, 19.5% Medium 199, 1% FCS) supplemented with 1% penicillin/streptomycin.

Plasmids—The region encoding amino acids 652–840 of human PMCA4b was amplified by 35 cycles of PCR (the conditions were denaturation at 94 °C for 45 s, annealing at 50 °C for 45 s, and extension at 72 °C for 1 min 30 s) using the oligonucleotides hPMCA4b652Sense (5′-TCTTCgCggATCCTgggACAATgAgAATgAgATC-3′) and hPMCA4b840Anti (5′-TCTTCCgCTCgAggATgCTgTCATAgACATTTCg-3′). The amplified product was digested with BamHI and XhoI and cloned into the BamHI-XhoI sites of plasmid pBT (Stratagene) to generate plasmid pBT-hPMCA4b (652–840).

pFlag-RASSF1A wild type and pFlag-RASSF1C (S61F) contain the cDNAs encoding human RASSF1A and RASSF1C, respectively, fused to the Flag epitope in a modified pcDNA3 vector in the manner previously reported (23). RASSF1C (S61F) cDNA was isolated from neurons derived from a cloned human teratocarcinoma cell line. The sequence of RASSF1C (S61F) is identical to that of the RASSF1C wild type protein (accession no. AF132676) except for a mutation in nucleotide 193 (C → T) that changes serine 61 to phenylalanine.

Site-directed mutagenesis (S131A) of RASSF1A was performed with a QuikChange kit (Stratagene, La Jolla, CA) using the protocol from the manufacturer. The oligomers used were: (5′-TgggAgACACCAgATCTTgCTCAAgCTgAgATTg-3′) and (5′-CAATCTCAgCTTgAgCAAgATCTggTgTCTCCCT-3′). Mutants were identified by the introduction of a silent BglII site and confirmed by sequencing.

pCMV-hPMCA4b contains the human PMCA4b cDNA and was a gift from Prof. E. Strehler (Department of Biochemistry and Molecular Biology, Mayo Clinic, Rochester, MN 55905).

To generate plasmids pGEX-KG-RASSF1C (50–123), pGEX-KG-RASSF1C (124–197), and pGEX-KG-RASSF1C (198–270), fragments encompassing nucleotides 159–380, 381–602, and 603–821 (numbering according to GenBank™ accession no. AF132676) were generated by 35 cycles of PCR (the conditions were denaturation at 94 °C for 30 s, annealing at 66 °C for 1 min, and extension at 72 °C for 1 min) using oligonucleotides BamRASSF1Sense50 (5′-TCTTCgCggATCCgACgAgCCTgTggAgTgggAg-3′) and XhoRASSF1Anti123 (5′-TCTTCCgCTCgAgTCCTgggCCCCgCCgggCATC-3′) for amplification of nucleotides 159 to 380, BamRASSF1Sense124 (5′-TCTTCgCggATCCCggggCACAAgTgTCAggCgC-3′) and XhoRASSF1Anti197 (5′-TCTTCCgCTCgAgCCgCAggggCTgCTCATCATC-3′) for amplification of nucleotides 381 to 602, and BamRASSF1Sense198 (5′-TCTTCgCggATCCCTgCggCTCCTggCAgggCCC-3′) and XhoRASSF1Anti270 (5′-TCTTCCGCTCGAGTCACCCAAGGGGGCAGGCGTG-3′) for amplification of nucleotides 603–821.

pFlag-RASSF1C (S61F) was used as template in the PCR reactions. Amplified fragments were cloned into the BamHI-XhoI sites of pGEX-KG to generate plasmids pGEX-KG-RASSF1C (50–123), pGEX-KG-RASSF1C (124–197), and pGEX-KG-RASSF1C (198–270), which encode GST fusion proteins containing RASSF1C (S61F) amino acids 50–123, 124–197, or 198–270, respectively.

To generate plasmids encoding Flag-tagged COOH-terminal deletion mutants of RASSF1C, fragments encompassing nucleotides 12–158, 12–269, 12–380, or 12–602 (numbering according to GenBank™ accession no. AF132676) were generated by 35 cycles of PCR (the conditions were denaturation at 94 °C for 30 s, annealing at 56 °C for 1 min, and extension at 72 °C for 1 min) using oligonucleotides EcoRASSF1Sense1 (5′-TCTTCCggAATTCCATgggCgAggCggAggCgCC-3′) and BamRASSF1Anti49 (5′-TCTTCgCggATCCTCACTggTCCCggCgCggCCTgC-3′), BamRASSF1Anti86 (5′-TCTTCgCggATCCTCACTTgTTCAAgCTCATgAAgAg-3′), BamRASSF1Anti123 (5′-TCTTCgCggATCCTCATCCTgggCCCCgCCgggCATC-3′), or BamRASSF1Anti197 (5′-TCTTCgCggATCCTCACCgCAggggCTgCTCATCATC-3′), respectively. pFlag-RASSF1C (S61F) was used as a template. Amplified products were digested with EcoRI and BamHI and cloned into the EcoRI-BamHI sites of plasmid p3xFlag-CMV7.1 (Sigma-Aldrich). The resulting plasmids pFlag-RASSF1C (1–49), pFlag-RASSF1C (1–86), pFlag-RASSF1C (1–123), and pFlag-RASSF1C (1–197) encode Flag-tagged RASSF1C truncated proteins containing amino acids 1–49, 1–86, 1–123, and 1–197, respectively.

Likewise, to generate Flag-tagged RASSF1C NH_2-terminal deletion mutants, fragments encompassing nucleotides 195–821, 231–821, or 270–821 (according to accession no. AF132676) were generated by 35 cycles of PCR by using the following oligonucleotides: EcoRASSF1Sense62 (5′-TCTTCCggAATTCCCAAgCTgAgATTgAgCAgAAg-3′) and BamRASSF1Anti270 (5′-TCTTCgCggATCCTCACCCAAgggggCAggCgTg-3′) for amplification of nucleotides 195–821 (PCR conditions: denaturation at 94 °C for 45 s, annealing at 44 °C for 45 s, extension at 72 °C for 45 s); EcoRASSF1Sense74 (5′-TCTTCCggAATTCCgCCCAgATCAACAgCAACCTC-3′) and BamRASSF1Anti270 for amplification of nucleotides 231–821 (PCR conditions: denaturation at 94 °C for 45 s, annealing at 48 °C for 45 s, extension at 72 °C for 45 s); and EcoRASSF1Sense87 (5′-TCTTCCggAATTCCgACggTTCTTACACAggCTTC-3′) and BamRASSF1Anti270 for amplification of nucleotides 270–821 (PCR conditions: denaturation at 94 °C for 30 s, annealing at 56 °C for 1 min, extension at 72 °C for 1 min).

pFlag-RASSF1C (S61F) was used as template in the PCR reactions. Amplified products were digested with EcoRI and BamHI and cloned into the EcoRI-BamHI sites of plasmid p3xFlag-CMV7.1 (Sigma-Aldrich). The resulting plasmids, pFlag-RASSF1C (62–270), pFlag-RASSF1C (74–270), and pFlag-RASSF1C (87–270), encode Flag-tagged RASSF1C truncated proteins containing amino acids 62–270, 74–270, and 87–270, respectively.

To generate the plasmid pCMV-MycRASSF1A, the coding sequence for RASSF1A was subcloned from pFlag-RASSF1A into the BamHI and XhoI cloning sites of the expression vector pCMV-Tag 3B (Stratagene).

To generate plasmid pFlag-hPMCA4b (652–840), a cDNA fragment coding for the region of human PMCA4b encompassing amino acids 652–840, was generated by 35 cycles of PCR using the following oligonucleotides and PCR conditions: BamPMCA4bSense652 (5′-TCTTCgCggATCCgTgggACAATgAgAATgAgATCC-3′) and XhoPMCA4bAnti840 (5′-TCTTCCgCTCgAgTCAgATgCTgTCATAgACATTTCgT-3′) (PCR conditions: denaturation at 94 °C for 45 s, annealing at 58 °C for 1 min,

extension at 72 °C for 1 min 30 s). The amplified fragment was digested with BamHI and XhoI and cloned into the BglII-XhoI restriction sites of plasmid p3xFlag-CMV7.1 (Sigma-Aldrich). To generate construct pFlag-hPMCA4b (749–840), the PCR fragment was digested with HindIII and XhoI and cloned into the HindIII-XhoI sites of plasmid p3xFlag-CMV7.1 (Sigma-Aldrich).

To clone pEGFP-R (50–123), the fragment encompassing nucleotides 159–380 of RASSF1C was amplified by 35 cycles of PCR using the oligonucleotides EcoRASSF1Sense50 (5′-TCTTCCggAATTCCgACgAgCCTgTggAgTgggAg-3′) and BamRASSF1Anti123 (5′-TCTTCgCggATCCTCATCCTgggCCCCgCCgggCATC-3′). PCR conditions were denaturation at 94 °C for 30 s, annealing at 66 °C for 30 s, and extension at 72 °C for 30 s. pFlag-RASSF1C (S61F) was used as a template in the PCR reactions. Amplified products were digested with EcoRI and BamHI and cloned into the EcoRI-BamHI sites of plasmid pEGFP-C1 (Clontech).

The fidelity of all amplified products was confirmed by sequencing.

pFA2-Elk1 (Stratagene) encodes a fusion protein between the DNA binding domain of the yeast Gal4 protein and the transactivation domain of the transcription factor Elk1. pFR-Luc (Stratagene) is a reporter vector containing a synthetic promoter with five tandem repeats of the yeast Gal4-binding sites that control the expression of the luciferase gene.

Two-hybrid Assay—A two-hybrid screen of a BacterioMatch™ human fetal heart cDNA library (Stratagene) was performed according to the instructions of a BacterioMatch™ two-hybrid system vector kit (Stratagene). Approximately 2×10^6 independent cDNA clones (which is equivalent to the whole library) were screened and assayed for resistance to carbenicillin or for β-galactosidase expression. To test for resistance to carbenicillin, transformed bacteria were plated onto LB-CTCK (250 μg/ml carbenicillin, 15 μg/ml tetracycline, 34 μg/ml chloramphenicol, 50 μg/ml kanamycin) agar plates and incubated at 30 °C for 48 h. To test for β-galactosidase expression, carbenicillin-resistant bacteria were plated onto LB-X-gal indicator plates (15 μg/ml tetracycline, 34 μg/ml chloramphenicol, 50 μg/ml kanamycin, 80 μg/ml X-gal, 200 μM phenylethyl-β-D-thiogalactoside) and incubated at 30 °C for 48 h.

Positive clones were sequenced following standard procedures.

Immunofluorescence Experiments—Primary rat neonatal cardiomyocytes were washed with PBS, warmed at 37 °C, and fixed with 2% paraformaldehyde for 30 min at room temperature. After two washes with PBS, cardiomyocytes were permeabilized with 0.1% Triton X-100 in PBS for 15 min. Unspecific staining was reduced by blocking with 10% horse serum for 30 min. Cells were incubated overnight with a 1% (v/v) solution of 5F10 anti-PMCA monoclonal antibody (Neomarkers) in 1% horse serum, and a 2% (v/v) solution of a goat polyclonal anti-RASSF1 antiserum (C-12, Santa Cruz) in 1% horse serum, and then washed three times with PBS. Antibody binding was detected by incubation, for 2 h in the dark, with a 1% (v/v) solution of a FITC-conjugated AffiniPure donkey anti-mouse IgG (Jackson ImmunoResearch) in 1% horse serum for detection of PMCA, and a 1% (v/v) solution of Texas Red-conjugated AffiniPure rabbit anti-goat IgG (Jackson ImmunoResearch) in 1% horse serum for detection of RASSF1. Unbound antibody was removed by washing three times with PBS.

HEK 293 cells were plated onto 22 × 22-mm coverslips at a density of 5×10^5 cells/coverslip. Transfected cells were washed with PBS, warmed at 37 °C, and fixed with 2% paraformaldehyde for 30 min at room temperature. Cells were washed twice with PBS and permeabilized with 0.1% Triton X-100 in PBS for 15 min. Unspecific staining was reduced by blocking with 10% horse serum for 30 min. Cells were incubated overnight with a 0.1% (v/v) solution of a rabbit polyclonal anti-PMCA4 antibody (Swant) in 1% horse serum and a 0.1% solution of a FITC-conjugated anti-Flag monoclonal antibody (Sigma) in 1% horse serum. Following incubation, cells were washed three times with PBS. Antibody binding to PMCA4 was detected by incubation for 2 h in the dark with a 1% (v/v) solution of a Texas Red dye-conjugated AffiniPure donkey anti-rabbit (Jackson ImmunoResearch) in 1% horse serum.

Unbound antibody was removed by washing three times with PBS.

Coverslips were mounted in Antifade reagent (Molecular Probes) on glass slides. Fluorescence was visualized using a Leica DM LB fluorescence microscope.

GST Fusion Protein Expression and Pull-down Assays—GST-RASSF1 fusion proteins were expressed in bacteria by incubation in LB medium supplemented with 1 mM isopropyl-1-thio-β-D-galactopyranoside and ampicillin (100 μg/ml), at 37 °C, for 5 h. Bacterial pellet was resuspended and sonicated in NET-N buffer (20 mM Tris, pH 8.0, 100 mM NaCl, 1 mM EDTA, pH 8.0, 20 μM PMSF, 500 ng/ml leupeptin, 1.0 μg/ml aprotinin, 500 ng/ml pepstatin). GST fusion proteins were purified by incubation with glutathione-agarose beads (Sigma) at 4 °C, for 45 min. After washing three times with NET-N buffer, beads containing purified GST fusion proteins were resuspended in RIPA buffer (1× PBS, 1% Igepal, 0.5% sodium deoxycholate, 0.1% SDS, 20 μM PMSF, 500 ng/ml leupeptin, 1.0 μg/ml aprotinin, 500 ng/ml pepstatin). Protein concentration and integrity were detected by PAGE electrophoresis and subsequent Coomassie Blue staining.

For pull-down assays, cardiac protein extracts were prepared by homogenization of mouse hearts in RIPA buffer (1 ml/heart). Cardiac protein extracts were precleared by incubation (4 °C, 60 min) with glutathione-agarose beads (100 μl of agarose beads/1 ml of cardiac extracts) to avoid unspecific binding. After preclearing, 250 μg of cardiac proteins were incubated with 3 μg of GST fusion protein-agarose beads at 4 °C, overnight. Beads were collected by centrifugation at 3,000 rpm, washed twice with RIPA buffer, and resuspended in 60 μl of 2× Laemmli loading buffer. Pulled down proteins were detected by Western blot.

Transient Transfection—For immunofluorescence assays, HEK 293 cells were plated in 22 × 22-mm coverslips at a density of 5×10^5 cells/coverslip the day before transfection. Cells were transfected with 6 μg of pCMV-hPMCA4b and 6 μg of pFlag-RASSF1A by using LipofectAMINE 2000 reagent (Invitrogen) according to the instructions from the manufacturer.

For immunoprecipitation experiments, HEK 293 cells were plated in 100 × 20-mm tissue culture dishes (4.5×10^6 cells/plate) the day before transfection. Cells were transfected in 4 ml of DMEM plus 10% FCS using 10 μg of the indicated expression plasmids by the calcium phosphate method. HEK 293 cells were incubated with precipitated DNA for 4.5 h, washed with PBS and incubated for 36 h more at 37 °C in 5 ml of DMEM plus 10% FCS prior to immunoprecipitation.

For luciferase assays, HEK 293 cells were plated in 6-well tissue culture plates (7×10^5 cells/well) the day before transfection. Cells were transfected with 3.0 μg of an expression vector encoding human PMCA4b (pCMV-hPMCA4b) or the corresponding empty vector (pcDNA3), 3.0 μg of an expression vector encoding RASSF1 (pFlag-RASSF1A wild type, pFlag-RASSF1A (S131A), or pFlag-RASSF1C (S61F)) or the corresponding empty vector (pcDNA3-Flag), 0.25 μg of pFA2-Elk1 (Stratagene), and 0.25 μg of the luciferase reporter pFR-Luc (Stratagene) by using LipofectAMINE 2000 reagent (Invitrogen) according to the instructions form the manufacturer. When indicated pEGFP-R (50–123) or the corresponding empty vector (pEGFP-C1) was included in the transfection reaction. Transfected cells were incubated with DNA-LipofectAMINE complexes for 24 h, washed once with PBS, and then incubated overnight in 5 ml of fresh DMEM, 10% FCS. The next morning, transfected cells were stimulated with epidermal growth factor (Sigma) (10 ng/ml) and incubated 6 h more. Cell extracts were prepared, and luciferase activity was determined with a luciferase assay system (Promega). Transfection efficiency was normalized by co-transfection of plasmid pEF-LacZ carrying the β-galactosidase gene under the control of the *EF1α* promoter, and determination of β-galactosidase activity (24).

Immunoprecipitation—Transfected HEK 293 cells were lysed with 0.4 ml of RIPA buffer (1× PBS, 1% Igepal, 0.5% sodium deoxycholate, 0.1% SDS, 20 μM PMSF, 500 ng/ml leupeptin, 1.0 μg/ml aprotinin, 500 ng/ml pepstatin). To minimize unspecific binding, 1.2 ml of protein extracts were precleared by incubation with 200 μl of protein G-agarose beads (Roche) and 5 μl of anti-luciferase polyclonal antibody (1 mg/ml) (Promega) at 4 °C, for 1 h. Beads were removed by centrifugation at 3,000 rpm, and 550 μl of precleared extracts were incubated overnight with the corresponding immunoprecipitating antibodies and 40 μl of protein G-agarose beads, at 4 °C with shaking. Beads were recovered by centrifugation at 3,000 rpm and washed three times with 500 μl of RIPA buffer. Washed beads were resuspended in 75 μl of 2× Laemmli loading buffer and analyzed by Western blot.

Western Blot—Samples were boiled and resolved, under reducing conditions, by sodium dodecyl sulfate-polyacrylamide gel electrophoresis (6 or 12% polyacrylamide for human PMCA4b or Flag-tagged RASSF1 detection, respectively). The gels were transferred onto nitrocellulose membranes and blocked with 5% (w/v) skim milk solution in Tris-buffered saline (TBS) at 4 °C overnight. After being washed in TBS-T (TBS, 0.05% Tween 20), the membranes were incubated for 2 h at room temperature with a 0.1% (v/v) solution of JA3 monoclonal antibody (Neomarkers) in TBS-T for PMCA4b detection, or a 0.1% (v/v) solution of anti-Flag M2 peroxidase-conjugated monoclonal antibody (Sigma-Aldrich) in TBS-T, for Flag-epitope detection. The membranes were washed three times for 5 min with TBS-T; for PMCA4b detection, membranes were incubated for 2 h at room temperature with a 0.013% (v/v) solution of peroxidase-labeled goat anti-mouse immunoglobulins (Dako) in TBS-T and washed twice with TBS-T. Bound antibodies were detected with the ECL Western blotting detection reagents (Amersham Biosciences).

RESULTS

Bacterial Two-hybrid Screen Using as Bait Amino Acids 652–840 from Human PMCA4b—The involvement of the PMCA COOH-terminal domain in binding to PDZ domain-containing proteins has been well documented (15–21). The primary protein structure of PMCA comprises two large intracellular regions in addition to the COOH- and NH_2-terminal domains. We reasoned that these regions could be involved in molecular interactions with proteins different to those previously described. As a first step to address this hypothesis, we decided to identify proteins that would bind to the region 652–840 of the second intracellular loop of human PMCA4b. This region was chosen because of its high degree of homology in the other isoforms of PMCA (91, 89.9, and 90.4% amino acid identity with PMCA1, -2, and -3, respectively), as the study of its functionality might provide some insight into the general function of PMCAs. In this work we have focused on the characterization of the interaction between PMCA4b and RASSF1. Whether other isoforms of PMCA interact with RASSF1 through this region requires further studies.

The plasmid pBT-hPMCA4b (652–840), expressing a protein containing the fragment 652–840 of PMCA4b fused to the full-length bacteriophage λcI repressor protein, was used as bait to screen a BacterioMatch™ human fetal heart cDNA library (Stratagene). The screening of 2×10^6 independent clones yielded positive clones resistant to carbenicillin and expressing β-galactosidase. We and others have previously suggested a role for PMCA as a modulator of signal transduction pathways via interaction with signaling target proteins such as members of the MAGUK family (15, 16), nNOS (19), or CASK (20). Hence, positive clones isolated by two-hybrid screening were sequenced, and further selected on the basis of their potential involvement in signal transduction pathways in cardiac cells. Clone A37 encoded a truncated protein corresponding to the region encompassing amino acids 120–344 of the tumor suppressor protein RASSF1E (accession no. AF102772). RASSF1 has recently been characterized as a Ras effector protein strongly expressed in the heart (23). The Ras pathway has been shown to be activated in cardiac hypertrophy and failure (25). Conversely activated Ras overexpression has been demonstrated to promote cardiac hypertrophy (26). In view of the potential role of PMCA4b as a signal transduction modulator, the identification of a Ras effector in our interaction screen was of particular interest. This formed the basis of our decision to investigate the molecular interaction between PMCA4b and RASSF1.

RASSF1E is one of at least seven splice variants (1A–1G) generated by alternative splicing and different promoter usage of the RASSF1 gene; 1A and 1C are the two major splice variants (22, 23). The region of RASSF1E that was pulled down with PMCA4b contains four amino acids, PILQ (positions 120–123), which are exclusive to this isoform. The remaining domain corresponds to an identical region shared with 1A and 1C (amino acids 120–340 in RASSF1A, 50–270 in RASSF1C) (Fig. 1). This result therefore suggests that both major isoforms, 1A and 1C, may in fact interact with human PMCA4b.

Co-precipitation of Human PMCA4b and Human Splice Variants RASSF1A and RASSF1C in Mammalian Cells—To confirm the interaction between PMCA4b and RASSF1 in mammalian cells, we co-transfected HEK 293 cells with the expression plasmids pCMV-hPMCA4b (encoding human PMCA4b) and pFlag-RASSF1A (for RASSF1A). Protein extracts were immunoprecipitated with the anti-PMCA monoclonal antibody 5F10. 5F10 was able to co-precipitate PMCA

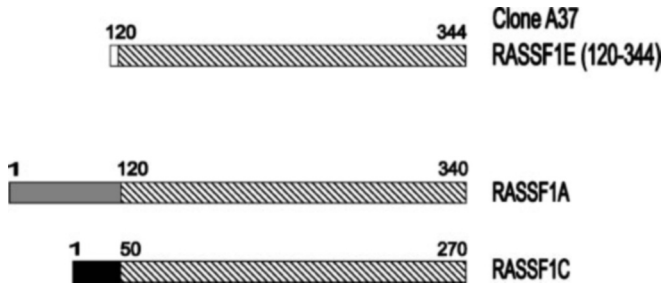

FIG. 1. **Identification of RASSF1 as a PMCA4b interaction partner.** The region 652–840 from hPMCA4b was used as bait in a two-hybrid experiment. One clone, A37, isolated based on its resistance to carbenicillin and its β-galactosidase expression, encoded a truncated version corresponding to amino acid residues 120–344 of the human RASSF1E protein. The sequence of this truncated protein is compared with those of the two major RASSF1 isoforms (RASSF1A and RASSF1C). *Hatched boxes* represent identical regions in the RASSF1 sequence pulled out by the two-hybrid screen, and isoforms 1A and 1C. *Gray* and *black boxes* show the divergent NH_2-terminal regions of RASSF1A or 1C, respectively. The numbering is according to accession nos. AF102770, AF132676, and AF102772 for RASSF1A, -1C, and -1E, respectively. The *white box* represents 4 amino acid residues (PILQ) that are exclusive to isoform 1E.

together with Flag-tagged RASSF1A (Fig. 2*A*). When cells were transfected with the pcDNA3-Flag empty vector, the 5F10 antibody precipitated PMCA but not the control Flag protein, demonstrating the specificity of the interaction (Fig. 2*A*). Control immunoprecipitations carried out with an irrelevant antibody (anti-luciferase) precipitated no protein at all, confirming the selectivity of the interaction (Fig. 2*A*).

Serine 131 in RASSF1A (61 in RASSF1C) has been reported to play a key role in the functionality of the protein (27). This residue is part of the motif WETPDL**S**QAEIEQK (amino acids 125–138 in RASSF1A, 55–68 in RASSF1C), which matches the ATM family phosphorylation consensus sequence (28). Mutation of serine 131 to phenylalanine has been shown to inhibit both phosphorylation and RASSF1A-mediated growth arrest (27). We therefore investigated whether mutation of serine 131 (61 in RASSF1C) had any effect on the interaction of RASSF1 with PMCA4b. For this purpose, we created by site-directed mutagenesis a mutant version of RASSF1A by substitution of serine 131 to alanine, RASSF1A (S131A). We also isolated from a human teratocarcinoma cell line a cDNA encoding a mutant version of RASSF1C with a substitution of serine 61 to phenylalanine, RASSF1C (S61F).

Immunoprecipitation experiments performed in transfected HEK 293 cells demonstrated that both RASSF1A wild type and S131A mutant proteins interacted with human PMCA4b (Fig. 2*B*). Likewise, RASSF1C (S61F) mutant co-precipitated with human PMCA4b (Fig. 2*B*), confirming our initial prediction of an interaction between PMCA4b and RASSF1C as well as RASSF1A. Interaction of PMCA4b and the mutant versions of RASSF1 suggests that serine 131 (61 in 1*C*), and therefore RASSF1 phosphorylation, is not required for association with PMCA4b. Untransfected cells and cells transfected with the pcDNA3-Flag empty vector were used as negative controls of the experiments (Fig. 2*B*).

In summary, these results show a physical interaction between PMCA4b and the two major splice variants of RASSF1, and demonstrate in a mammalian context our initial observation from two-hybrid experiments.

PMCA and RASSF1 Co-localize in Mammalian Cells—To further substantiate the physical interaction between PMCA and RASSF1 in mammalian cells, we co-transfected HEK 293 cells with the expression plasmids pCMV-hPMCA4b and pFlag-RASSF1A, and analyzed the localization of the recombinant proteins by immunofluorescence. Ectopic PMCA4b and Flag-

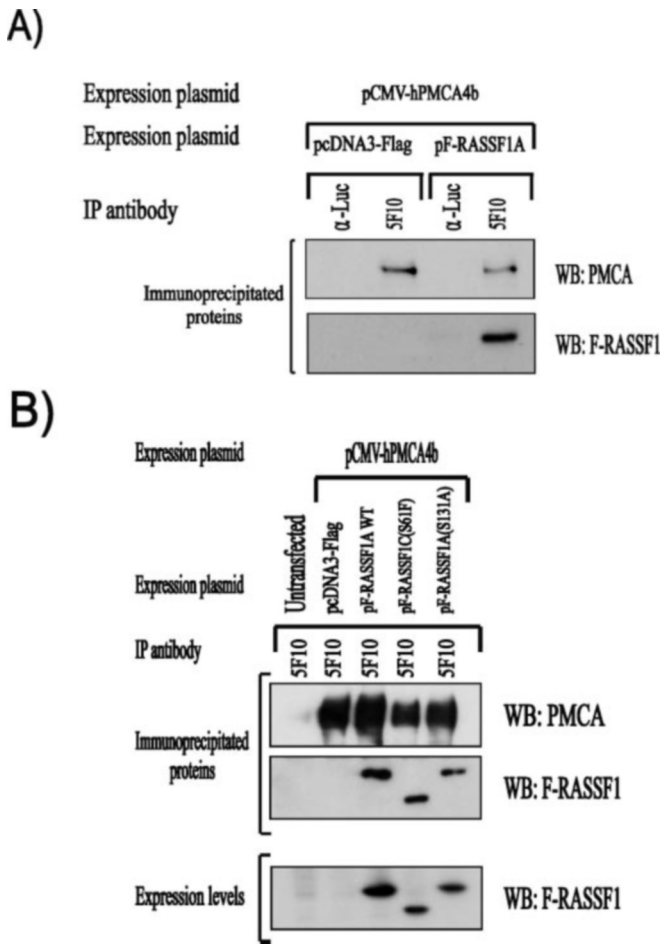

FIG. 2. **Human PMCA4b and RASSF1 interact in mammalian cells.** PMCA and Flag-RASSF1 co-precipitate by using a monoclonal antibody directed against PMCA, demonstrating the physical interaction between the two proteins. *A*, expression vectors encoding human PMCA4b (pCMV-hPMCA4b) and a Flag-tagged version of human RASSF1A (pF-RASSF1A) were co-transfected in HEK 293 cells. Protein lysates were incubated with an anti-PMCA monoclonal antibody (5F10) or an irrelevant antibody raised against firefly luciferase (α-Luc), and subsequently protein complexes precipitated with protein G beads. Western blots of immunoprecipitated proteins were probed with the JA3 anti-PMCA4b monoclonal antibody or the M2 anti-Flag monoclonal antibody, to detect PMCA4b (*WB: PMCA*) or Flag-tagged RASSF1 (*WB: F-RASSF1*), respectively. Western blot of cells transfected with empty vector (pcDNA3-Flag) was used as negative control. *B*, expression vectors encoding human PMCA4b (pCMV-hPMCA4b) and a Flag-tagged version of human RASSF1A wild type (pF-RASSF1A), a functionally defective mutant of RASSF1A (pF-RASSF1A (S131A)), or a functionally defective mutant of RASSF1C (pF-RASSF1C (S61F)), were co-transfected in HEK 293 cells. Protein lysates were incubated as described above and analyzed by Western blot. *WB: PMCA*, detection of PMCA4b; *WB:F-RASSF1*, detection of Flag-tagged RASSF1 proteins. Cells left untransfected, and transfections performed with empty vector (pcDNA3-Flag) were used as negative controls. RASSF1 mutants co-precipitated together with PMCA4b, suggesting that serine 131 of RASSF1A (61 in RASSF1C) is not essential for interaction.

RASSF1A were detected by staining with a polyclonal antibody that specifically recognizes PMCA4 (Swant) and an anti-Flag monoclonal antibody (Sigma), respectively. PMCA4b was localized in transfected cells, at the plasma membrane and forming a meshwork-like pattern in the cytoplasm (Fig. 3*A*). RASSF1 showed a similar pattern, localizing at the plasma membrane and in a cytoplasmic meshwork (Fig. 3*A*). The merged image showed co-localization of ectopic PMCA4b and Flag-RASSF1A (Fig. 3*A*). Samples incubated only with secondary antibodies, FITC-conjugated anti-mouse IgG, or Texas Red-conjugated anti-rabbit IgG did not show any staining (data not shown), confirming the specificity of the immunofluorescence detection.

Likewise, we analyzed the subcellular localization of the endogenous proteins in primary rat neonatal cardiomyocytes by immunofluorescence. PMCA4 and RASSF1 were detected by staining with 5F10 (a monoclonal antibody that recognizes all PMCA isoforms), and a polyclonal antiserum raised against RASSF1, respectively. Endogenous PMCA and RASSF1 also showed co-localization at the plasma membrane and in a cytoplasmic network (Fig. 3*B*). No staining at these cellular organelles was detected in control samples incubated only with secondary antibodies, FITC-conjugated anti-mouse IgG, or Texas Red-conjugated anti-goat IgG (Fig. 3*B*). These results confirm the physical interaction between endogenous PMCA and RASSF1. The strong fluorescence detected in the perinuclear areas of rat neonatal cardiomyocytes cells appears to be unspecific, as control samples stained only with the secondary antibodies also showed staining in these areas (Fig. 3*B*).

Taken together, these results strongly suggest the physical association of PMCA4 and RASSF1 in mammalian cells.

The Region 74–123 of RASSF1C Is Essential for Interaction with PMCA4b—Our next aim was to determine the domain of RASSF1 involved in the interaction with PMCA4b. The results from two-hybrid and immunoprecipitation experiments indicated that the RASSF1 interaction domain should be found in the identical region shared by isoforms 1A and 1C. Therefore, we generated GST fusion proteins containing amino acids 50–123, 124–197, or 198–270 of RASSF1C (S61F) (Fig. 4*A*) and used them in GST pull-down assays together with protein extracts isolated from mouse hearts. GST-RASSF1C (50–123) pulled down endogenous cardiac PMCA4 (Fig. 4*B*). PMCA4, however, did not interact with GST fusion proteins containing regions 124–197 or 198–270 of RASSF1C (Fig. 4*B*), indicating that the interaction domain was included within the region 50–123. Absence of interaction in control reactions performed with empty or GST-bound glutathione-agarose beads demonstrated the specificity of the assay (Fig. 4*B*).

To confirm and further characterize the RASSF1 domain implicated in the interaction with PMCA, we generated a series of Flag-tagged RASSF1C (S61F) COOH-terminal deletion mutants (Fig. 4*C*) and assayed by immunoprecipitation their capacities to interact with human PMCA4b. HEK 293 cells were co-transfected with pCMV-hPMCA4b and plasmid pFlag-RASSF1C (1–270), pFlag-RASSF1C (1–197), pFlag-RASSF1C (1–123), pFlag-RASSF1C (1–86), or pFlag-RASSF1C (1–49), and protein extracts were immunoprecipitated with the anti-PMCA monoclonal antibody 5F10. Deletion of the regions 198–270 or 124–270 of RASSF1C had no effect on the binding of the RASSF1C mutants to PMCA4b, as 5F10 co-precipitated PMCA4b and the corresponding RASSF1C truncated proteins (Fig. 4*D*, *upper panel*). However, removal of the region 87–270 in the mutant Flag-RASSF1C (1–86) significantly inhibited the interaction with PMCA, although a minimal association was still present (Fig. 4*D*, *upper panel*). Further deletion of amino acids 50–86 in the mutant Flag-RASSF1C (1–49) totally impaired its interaction with PMCA4b (Fig. 4*D*, *upper panel*). Immunoprecipitations carried out with an irrelevant antibody (anti-luciferase) precipitated no protein at all (data not shown), demonstrating the specificity of the interaction. Untransfected cells or cells transfected with the pFlag empty vector were used as negative controls (Fig. 4*D*). The Flag-tagged RASSF1C (1–49) mutant was expressed at levels higher than those of the Flag-RASSF1C (1–270) full-length protein, ruling out the possibility of poor expression as the reason for lack of interaction (Fig. 4*D*, *lower panel*).

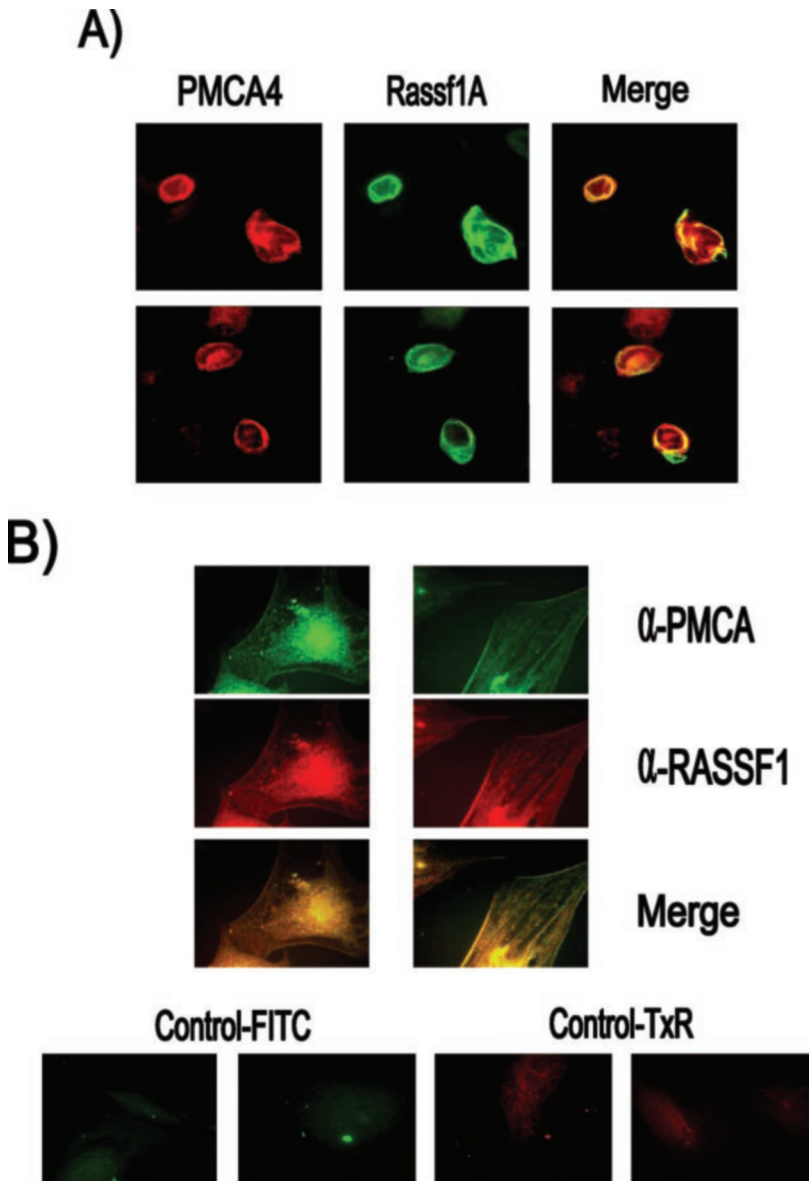

FIG. 3. **RASSF1 and PMCA co-localize in mammalian cells.** Double immunofluorescence staining of PMCA and RASSF1 shows co-localization in mammalian cells. *A*, HEK 293 cells were co-transfected with the expression vectors pCMV-hPMCA4b and pFlag-RASSF1A. The localization of the resulting PMCA4b or Flag-tagged RASSF1A proteins was detected by incubation with a rabbit polyclonal anti-PMCA4 antiserum (Swant) (*left panel*) or a FITC-conjugated anti-Flag monoclonal antibody (Sigma) (*middle panel*), respectively. Bound anti-PMCA4 antibodies were stained by secondary incubation with a Texas Red dye-conjugated AffiniPure donkey anti-rabbit IgG. The merged image (*right panel*) shows co-localization of PMCA4 and RASSF1A at the plasma membrane and forming a meshwork-like pattern in the cytoplasm. Two representative fields containing transfected cells are shown. *B*, the localization of endogenous PMCA and RASSF1 proteins was detected by incubating rat neonatal cardiomyocytes with the 5F10 anti-PMCA monoclonal antibody (*α-PMCA*) and an anti-RASSF1 goat polyclonal antibody (*α-RASSF1*), respectively. Bound antibodies were stained by secondary incubation with FITC-conjugated AffiniPure donkey anti-mouse IgG or a Texas Red dye-conjugated AffiniPure rabbit anti-goat IgG, for detection of PMCA, or RASSF1, respectively. The merged image shows co-localization of PMCA and RASSF1 at the plasma membrane and in a cytoplasmic meshwork structure, suggesting the physical interaction of the endogenous proteins. Control experiments incubated only with secondary antibodies (*lower panel*) confirmed the specificity of the immunofluorescence detection.

These results indicate that the region encompassing amino acids 87–123 plays a major role in the interaction, although some residues upstream of amino acid 86 must still be involved in the association with PMCA4b and be required for a maximal interaction.

To investigate this hypothesis, we prepared a series of NH_2-terminal deletion mutants (Fig. 4*C*) and tested their capabilities for binding to PMCA4b by immunoprecipitation as previously described. Deletion of the region 1–61 or 1–73 of RASSF1C did not alter the binding of mutants Flag-RASSF1C (62–270) or Flag-RASSF1C (74–270) to PMCA4b (Fig. 4*E*, *upper panel*). Further removal of the amino acids 74–86 in the mutant Flag-RASSF1C (87–270) resulted in a slight, but significant reduction in its interaction with PMCA4b (Fig. 4*E*, *upper panel*), indicating that the region 74–86 is required for maximal interaction between the two proteins. Levels of the Flag proteins prior to immunoprecipitation were checked by Western blot to eliminate ascribing differences to differential expression (Fig. 4*E*, *lower panel*).

In summary, these results demonstrate that the region 74–123 of RASSF1C is required for a maximal interaction with PMCA4b.

The Region 652–748 of PMCA4b Is Critical for Interaction with RASSF1—The two-hybrid assay showed that the region 652–840 of PMCA4b was sufficient to mediate the interaction with RASSF1. To confirm this result and identify the minimal domain of PMCA4b that interacts with RASSF1, we generated plasmids pFlag-hPMCA4b (652–840) and pFlag-hPMCA4b (749–840) encoding Flag-tagged proteins containing the regions 652–840 and 749–840, respectively (Fig. 5*A*) of the human PMCA4b protein. HEK 293 cells were co-transfected with plasmid pCMV-MycRASSF1A (encoding a Myc-tagged version of RASSF1A) and plasmid pFlag-hPMCA4b (652–840) or pFlag-hPMCA4b (749–840). Protein extracts isolated from transfected cells were immunoprecipitated with an anti-Myc monoclonal antibody (Invitrogen), and immunoprecipitated proteins detected by Western blot (Fig. 5*B*, *left panel*). As expected, Flag-PMCA4b (652–840) co-precipitated with RASSF1A. However, Flag-PMCA4b (749–840) lacking the region 652–748 of hPMCA4b failed to interact with RASSF1A, suggesting that the missing region is critical for the interaction of human PMCA4b and RASSF1A. Immunoprecipitations carried out with an irrelevant antibody (anti-luciferase) precipitated no protein at all (data not shown), demonstrating the specificity of the interaction. Cells left untransfected were used as a negative control. Expression of Flag proteins was detected

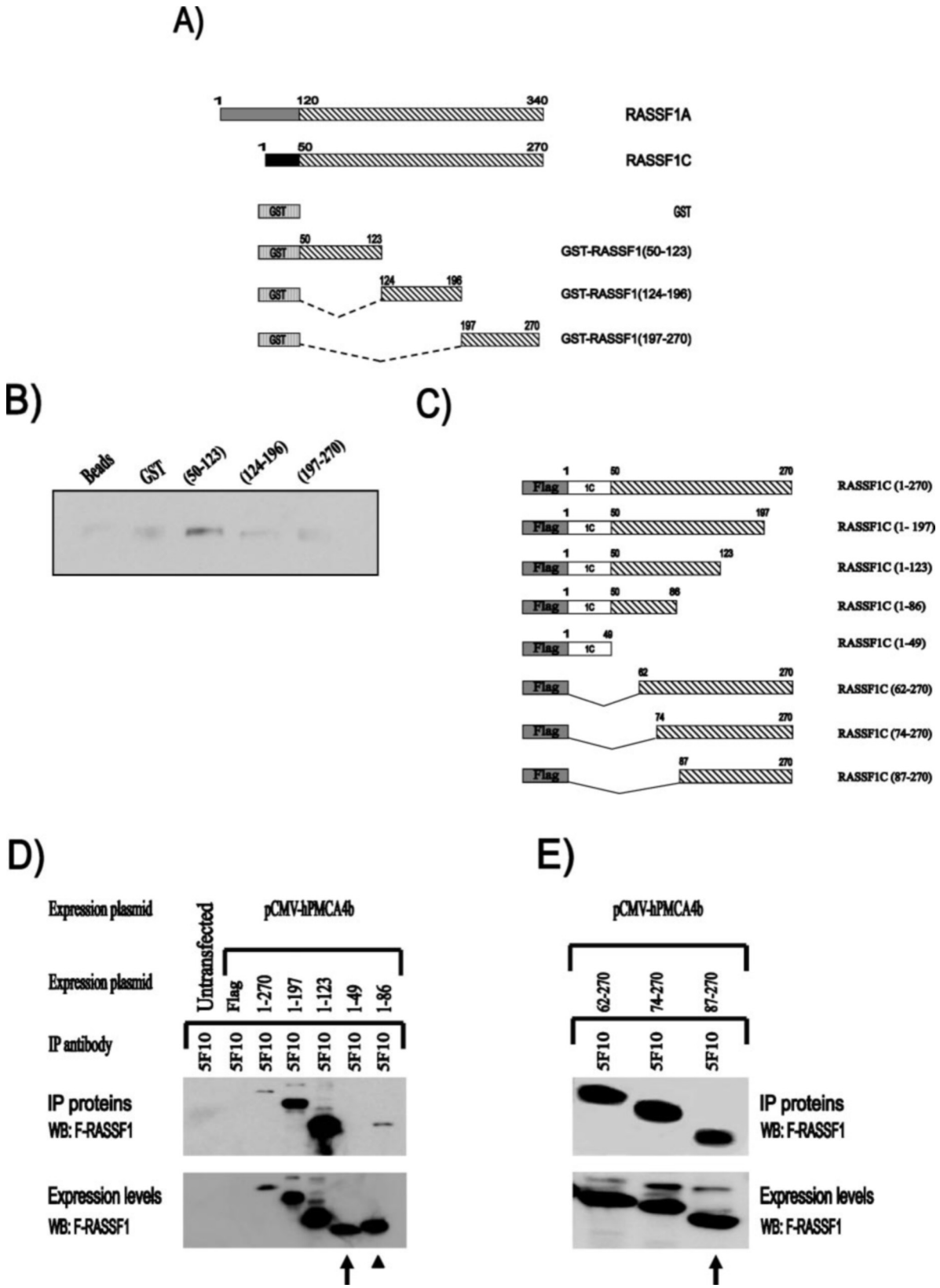

FIG. 4. **Interaction with PMCA maps to the region 75–123 of RASSF1C.** *A*, schematic representation of GST-RASSF1C fusion proteins used for pull-down assays. *Hatched boxes* represent identical regions in RASSF1A and RASSF1C. The *numbers* correspond to RASSF1C amino acids according to accession no. AF132676. *B*, GST-RASSF1 pull-down assay performed by incubating 250 μg of cardiac proteins with 3 μg of GST fusion protein-agarose beads. Pulled-down proteins were identified by Western blot using a 1:1000 dilution of an anti-PMCA4 polyclonal antibody (Swant) in 5% skim milk TBS-T. Control reactions were performed by using agarose beads either empty (*beads*) or coupled to native GST (*GST*). *(50–123)*, *(124–196)*, and *(197–270)* denote pull-down reactions carried out with GST fusion proteins containing the regions 50–123, 124–196, and 197–270, respectively, of RASSF1C. *C*, schematic representation of Flag-tagged RASSF1C COOH- or NH_2-terminal deletion mutants used for immunoprecipitation. *Hatched boxes* represent identical regions in RASSF1A and RASSF1C. *White boxes* represent the unique RASSF1C NH_2-terminal domain. The *numbers* correspond to RASSF1C amino acids according to accession no. AF132676. *D*, expression vectors encoding hPMCA4b (pCMV-hPMCA4b) or Flag-tagged COOH-terminal deletion mutants of RASSF1C encoding amino acids 1–197, 1–123, 1–86, or 1–49, were

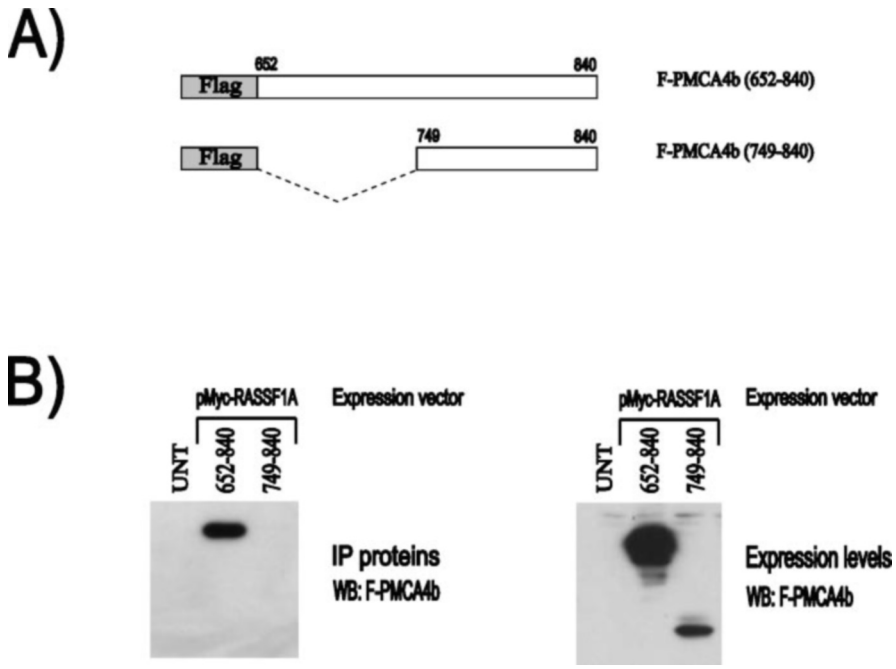

FIG. 5. **Interaction with RASSF1 requires the region 652–748 of human PMCA4b.** *A*, schematic representation of Flag-tagged proteins used for immunoprecipitation. *White boxes* indicate the region of PMCA4b that has been fused to the Flag tag. The *numbers* correspond to human PMCA4b amino acids according to accession no. NM_001684. *B*, immunoprecipitation analysis of the interaction between RASSF1A and Flag-tagged proteins containing the regions 652–840 or 749–840 of PMCA4b. Expression vectors encoding Myc-RASSF1A (pCMV-MycRASSF1A) and Flag-tagged PMCA4b (625–840) or PMCA4b (749–840) were co-transfected in HEK 293 cells. Protein lysates were incubated with an anti-Myc monoclonal antibody (Invitrogen) and protein complexes precipitated with protein G beads. Untransfected cells were used as a negative control. Flag-tagged immunoprecipitated proteins were detected by Western blot with M2 anti-Flag peroxidase monoclonal antibody (*left panel*). The protein lacking the region 652–748 failed to co-precipitate with RASSF1, indicating the requirement of this region for the interaction. Expression levels of the Flag proteins prior to immunoprecipitation were analyzed by Western blot (*right panel*) with M2 anti-Flag peroxidase monoclonal antibody confirming the presence of Flag-tagged PMCA4b (749–840).

by Western blot (Fig. 5*B*, *right panel*), confirming the presence of Flag-PMCA4b (652–840) or Flag-PMCA4b (749–840) in the immunoprecipitation reactions.

PMCA4b/RASSF1 Interaction Inhibits EGF-dependent Activation of Erk—The role of the signal transduction molecule Ras in the EGF-dependent activation of the Erk pathway in mammalian cells is well recognized (29). RASSF1 has been described as an effector of Ras that binds to its active form (Ras-GTP) (23). Therefore, we decided to investigate the functional consequences of the interaction between PMCA4b and RASSF1 on the activity of Erk in cells stimulated with EGF, using the PathDetect Elk1 *trans*-reporting system (Stratagene). This system is based on the analysis of the transcriptional activity of a reporter protein containing the DNA binding domain of the yeast Gal4 protein fused to the transactivation domain of the transcription factor Elk1. Determination of the transcriptional activity of the reporter provides an indirect indication of the activation status of the mitogen-activated protein kinase Erk. HEK 293 cells were transfected with the luciferase reporter vector pFR-Luc (Stratagene), and the expression plasmids pFA2-Elk1 (Stratagene), pCMV-hPMCA4b (for human PMCA4b expression), and/or pFlag-RASSF1A (for production of RASSF1A wild type). EGF stimulation of transfected cells enhanced luciferase activity between 30- and 60-fold. As shown in Fig. 6, ectopic expression of hPMCA4b or RASSF1A alone did not alter Gal4-Elk1 activation in response to EGF (Fig. 6). However, coexpression of both proteins caused a significant ($p \leq 0.05$) reduction in the EGF-mediated activation of the reporter, suggesting that the interaction of PMCA4b and RASSF1 partially inhibits the EGF-dependent activation of the Erk pathway (Figs. 6 and 7).

Confirming this hypothesis, when the RASSF1 functionally defective mutants RASSF1A (S131A) or RASSF1C (S61F) were used instead of the wild type protein, Elk activity was not significantly altered (Fig. 6). Furthermore, blocking PMCA4b/RASSF1 interaction with an excess of GFP-R (50–123), a GFP fusion protein containing the RASSF1 interaction domain, reversed the inhibition in the EGF-mediated activation of Gal4-Elk1, demonstrating the functionality of the interaction (Fig. 7). In fact, overexpression of GFP-R (50–123) not only reversed the inhibition because of ectopically expressed PMCA4b and RASSF1, but further increased

co-transfected in HEK 293 cells. *(1–270)* corresponds to the full-length protein. Protein lysates were incubated with an anti-PMCA monoclonal antibody (5F10) and protein complexes precipitated with protein G beads. Untransfected cells and empty vector (pcDNA3-Flag) were used as negative controls. Flag-RASSF1 immunoprecipitated proteins were detected by Western blot with M2 anti-Flag peroxidase monoclonal antibody (*upper panel*). *Arrowhead* indicates the decrease in the interaction of mutant RASSF1 (1–86) (*upper panel*), and its expression levels (*lower panel*), indicating that the region 87–123 plays a major role in the interaction. *Arrow* denotes the absence of interaction of mutant RASSF1C (1–49) (*upper panel*), and its expression levels (*lower panel*). Expression levels of the Flag proteins prior to immunoprecipitation were analyzed by Western blot (*lower panel*) with M2 anti-Flag peroxidase monoclonal antibody, using 30 μl of protein extracts from cells transfected with plasmids pFlag-RASSF1C (1–270) (full-length) or pFlag-RASSF1C (1–49); 3 μl of extracts from cells transfected with pFlag-RASSF1C (1–197) or pFlag-RASSF1C (1–123); and 15 μl of extracts from cells transfected with pFlag-RASSF1C (1–86). *E*, immunoprecipitation analysis of the interaction between PMCA4b and a series of NH_2-terminal RASSF1C deletion mutants. Conditions were the same as indicated for the COOH-terminal mutants. *62–270*, *74–270*, and *87–270* indicate Flag-tagged proteins containing the regions 62–270, 74–270, and 87–270 of RASSF1C. *Arrow* denotes the slight decrease in interaction with PMCA4b of the mutant RASSF1C (87–270) (*upper panel*), and its expression levels (*lower panel*). Protein expression levels were analyzed as above, using 15 μl of protein extracts isolated from transfected cells.

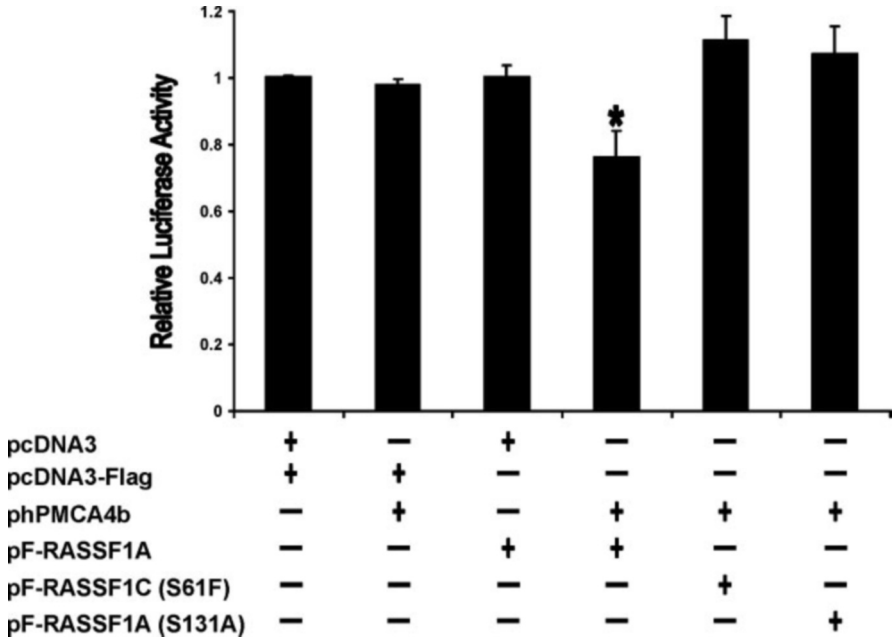

FIG. 6. **Co-expression of hPMCA4b and RASSF1 inhibits the Erk pathway.** 0.25 μg of expression vector pFA2-Elk1, 0.25 μg of luciferase reporter pRL-Luc, 3 μg of an expression vector encoding hPMCA4b (pCMV-hPMCA4b), and 3 μg of a vector producing Flag-tagged RASSF1A (wild type), Flag-RASSF1A (S131A) (a RASSF1A mutant version where serine 131 has been mutated to alanine), or Flag-RASSF1C (S61F) (a RASSF1C mutant version where serine 61 has been substituted to phenylalanine) were co-transfected in HEK 293 cells as described under "Experimental Procedures," and stimulated with epidermal growth factor (10 ng/ml). 6 h after stimulation, luciferase activity was measured. The EGF-dependent activation of the luciferase reporter when the empty vectors pcDNA3-Flag and pCDNA3 were co-transfected was taken as base line and assigned an arbitrary value of 1. The effects of expression of hPMCA4b, and/or RASSF1 wild type or mutant proteins, in the EGF-dependent activation of the reporter are expressed as luciferase activity relative to the base line. Transfection efficiency was normalized by co-transfection of the pEF-LacZ plasmid as internal control, and measure of β-galactosidase expression. *Asterisk* denotes statistically significant ($p \leq 0.05$, according to Student's *t* test) inhibition of the EGF-mediated activation of the Gal4-Elk1 reporter as a result of co-expression of hPMCA4b and RASSF1A wild type. Means ± S.E. of three independent experiments are shown.

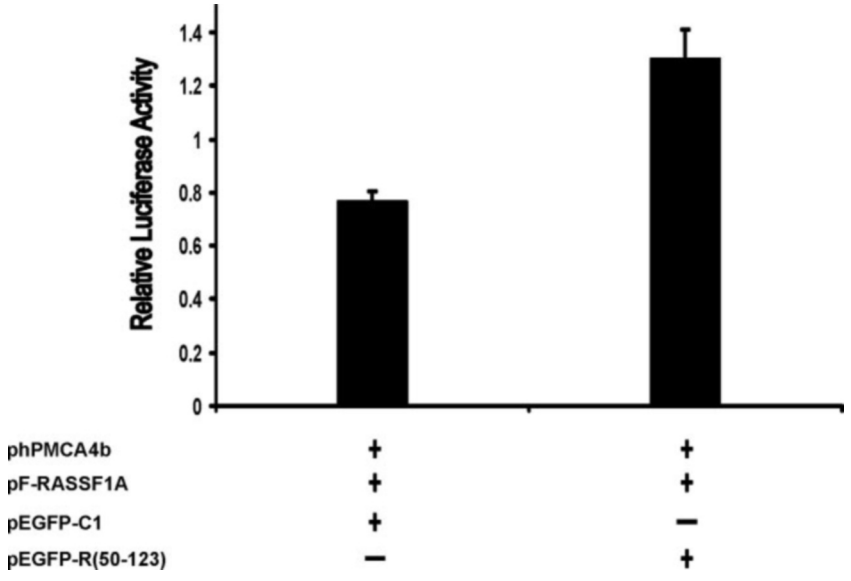

FIG. 7. **PMCA4b/RASSF1 interaction inhibits the Erk pathway.** Transfections, luciferase assays, and data representation were as described for Fig. 6, except that 6 μg of pEGFP-C1 (empty vector) or pEGFP-R (50–123) (a GFP protein containing the region 50–123 of RASSF1C (S61F)) were also included in the transfection reactions. Overexpression of an excess of EGFP-R (50–123) reversed the PMCA/RASSF1-mediated inhibition in the EGF-dependent activation of the Gal4-Elk1 reporter, whereas GFP overexpression did not have any effect. This result demonstrates the functionality of the interaction. Means ± S.E. of at least three independent experiments are shown.

the transactivation activity of the reporter (Fig. 7), suggesting that GFP-R (50–123) might eliminate some inhibition because of endogenous PMCA4b and RASSF1 proteins. No effect was observed in control experiments where native GFP protein was expressed in excess (Fig. 7).

In summary, these results demonstrate that the physical interaction between PMCA4b and RASSF1 exerts a negative modulatory role on EGF-activated Ras signaling pathways.

DISCUSSION

In this work, we describe a novel functional interaction between PMCA and the tumor suppressor protein RASSF1.

Either ectopically expressed or endogenous PMCA and RASSF1 co-localized in mammalian cells. RASSF1 localized at the plasma membrane and in a cytoplasmic meshwork. This meshwork-like pattern formed by RASSF1 in cardiac cells is identical to that reported by Liu *et al.* (30) in mammalian tissue culture cell lines, and has been reported to be a result of the association of RASSF1 with the microtubule network. PMCA co-localization suggests that it might also be associated with the cytoskeleton network (possibly for intracellular transport), and in fact, cytoplasmic detection of PMCA has been recently reported by Rivas *et al.* (31), who showed redistribution of PMCA4 from the cytoplasm to the plasma membrane upon T-cell activa-

tion. Moreover, preliminary experiments performed in our laboratory indicate interaction between PMCA and cardiac α-tubulin.[2] We are currently exploring this possibility.

We have determined that PMCA4b can interact with the two major splice variants of RASSF1, RASSF1A and -1C, and found that this interaction requires the region encompassing amino acids 652–748 of the catalytic domain of PMCA. Our work describes a novel protein-protein interaction involving a domain of PMCA other than the COOH terminus and suggests that PMCA could function as a molecular scaffold for the assembly of macromolecular complexes by recruiting several proteins through interactions with different domains.

The region of RASSF1 responsible for interacting with PMCA4b has been mapped within the domain 74–123 of RASSF1C (144–193 in RASSF1A). These regions are located within the identical domains shared by the two isoforms, which is in keeping with our results indicating that both isoforms interact with PMCA4b. In fact, the mutant Flag-RASSF1C (1–49), which failed to bind to PMCA4b, only contains the specific NH_2-terminal region of RASSF1C. Moreover, mapping of the interaction domain at the region 74–123 concurs with our finding that the integrity of the association with PMCA4b is unaffected by mutation of serine 61 in RASSF1C.

Ectopic expression of hPMCA4b or RASSF1A alone did not alter Erk activation in response to EGF. However, co-expression of both proteins significantly reduced the activity of an Erk-dependent luciferase reporter plasmid. The lack of effect observed when only one of the proteins is overexpressed can be explained as follows. First, endogenous levels of PMCA4b and RASSF1 are much lower in comparison to ectopically expressed protein (for example, see Fig. 2*B*). Second, the Erk inhibition fundamentally relies on the interaction between PMCA4b and RASSF1 as a complex at a physical level. Hence, for a given amount of complex between endogenous PMCA and RASSF1, the amount that is unbound and therefore available to ectopically overexpressed protein is negligible and overexpression of one protein alone will not lead to the formation of new complex.

PMCA and RASSF1 functionally interact at the endogenous level, leading to a certain degree of inhibition of Erk activity, as evidenced by the increase in reporter gene activity when the interaction domain is co-transfected (Fig. 7).

These results strongly suggest a functional role for the interaction between PMCA and RASSF1 in the regulation of the Erk pathway. Clearly, overexpression models performed in cultured cells represent a preliminary, but necessary step, in establishing hypotheses which can then be tested in a physiological setting. We are currently investigating the physiological relevance of the interaction between these two proteins *in vivo* using transgenic animal models.

RASSF1 has been implicated in Ras-dependent, caspase-mediated apoptosis (23), and several studies have indicated a role for PMCA in apoptosis (32–34). Our results demonstrate that interaction of PMCA4b and RASSF1 inhibits the activity of the Erk pathway, a signaling cascade critical for the regulation of cellular proliferation and survival (35). Therefore, one could speculate that PMCA functions as an organizer of a macromolecular complex involved in apoptotic signaling by inhibiting proliferation and promoting cell death. In this context, Bertin *et al.* have recently described two novel caspase recruitment domain (CARD)-containing proteins (CARD11 and CARD14) that belong to the MAGUK family (36). CARD is a protein module involved in apoptotic signaling through protein interactions (37). As is the case with other MAGUK family proteins, CARD11 and CARD14 contain PDZ domains (36), and may therefore interact with the COOH-terminal PDZ binding domain of PMCA. If this is the case, PMCA could recruit two proteins involved in apoptosis through interaction with two different domains. We are exploring this possibility further in our laboratory.

Our group and others have demonstrated the location of PMCA in caveolae (38, 39). In keeping with the role of PMCA as an assembler and potential regulator of Ca^{2+} in multiprotein complexes involved in apoptosis, caveolar microdomains have been suggested to mediate apoptosis. In fact, apoptosis induced by tumor necrosis factor-α has been proven to be dependent on intact caveolae (40), and the tumor necrosis factor-α receptor and caspase-3 co-localize in caveolar domains (40, 41). Furthermore, cleavage of PMCA pumps by caspases in cells undergoing apoptosis leads to the inactivation of PMCA and subsequent cellular necrosis (32, 33) although Paszty *et al.* (42) have shown recently that caspase cleavage of the PMCA increases its activity. In addition, antisense inhibition of PMCA has been reported to induce apoptosis (34).

RASSF1 belongs to a gene family of structurally related proteins characterized by the presence of a Ras association domain, including the human RASSF1–3 and Nore1 proteins (22, 23, 43, 44). When the sequence of the RASSF1 domain that interacts with PMCA4b was compared with the corresponding domain in RASSF2, we did not find any significant homology in that region. However, as well as RASSF1, human RASSF2 promotes apoptosis and cell cycle arrest (44). Interestingly, RASSF1 binds to H-Ras (23), whereas RASSF2 binds mainly to K-Ras and only interacts very weakly with H-Ras (44). Disruption of caveolae by expression of a dominant-negative caveolin has been reported to inhibit H-Ras- but not K-Ras-mediated signal transduction (45). Additionally, it is thought that H-Ras preferentially localizes to lipid rafts/caveolae, whereas K-Ras shows a less specific pattern of localization and it is found throughout the plasma membrane (46). This raises the attractive possibility of the specific involvement of caveolar PMCA in H-Ras-mediated signaling through association with RASSF1.

In summary, our results demonstrate a novel functional interaction between PMCA and RASSF1, suggesting a role for PMCA as an organizer, and potential regulator of Ca^{2+}, in macromolecular signal transduction complexes. Moreover, these results lead to new testable hypotheses of the molecular mechanisms involving PMCA in the regulation of apoptotic signaling.

[2] A. L. Armesilla, J. C. Williams, and L. Neyses, unpublished results.

REFERENCES

1. Strehler, E. E., and Zacharias, D. A. (2001) *Physiol. Rev.* **81,** 21–50
2. Pedersen, P. L., and Carafoli, E. (1987) *Trends Biochem. Sci.* **12,** 146–150
3. Pedersen, P. L., and Carafoli, E. (1987) *Trends Biochem. Sci.* **12,** 186–189
4. Shull, G. E., and Greeb, J. (1988) *J. Biol. Chem.* **263,** 8646–8657
5. Greeb, J., and Shull, G. E. (1989) *J. Biol. Chem.* **264,** 18569–18576
6. Verma, A. K., Filoteo, A. G., Stanford, D. R., Wieben, E. D., Penniston, J. T., Strehler, E. E., Fischer, R., Heim, R., Vogel, G., and Mathews, S. (1988) *J. Biol. Chem.* **263,** 14152–14159
7. Strehler, E. E., James, P., Fischer, R., Heim, R., Vorherr, T., Filoteo, A. G., Penniston, J. T., and Carafoli, E. (1990) *J. Biol. Chem.* **265,** 2835–2842
8. Heim, R., Iwata, T., Zvaritch, E., Adamo, H. P., Rutishauser, B., Strehler, E. E., Guerini, D., and Carafoli, E. (1992) *J. Biol. Chem.* **267,** 24476–24484
9. Brown, B. J., Hilfiker, H., DeMarco, S. J., Zacharias, D. A., Greenwood, T. M., Guerini, D., and Strehler, E. E. (1996) *Biochim. Biophys. Acta* **1283,** 10–13
10. Keeton, T. P., and Shull, G. E. (1995) *Biochem. J.* **306,** 779–785
11. James, P., Maeda, M., Fischer, R., Verma, A. K., Krebs, J., Penniston, J. T., and Carafoli, E. (1988) *J. Biol. Chem.* **263,** 2905–2910
12. Enyedi, A., Vorherr, T., James, P., McCormick, D. J., Filoteo, A. G., Carafoli, E., and Penniston, J. T. (1989) *J. Biol. Chem.* **264,** 12313–12321
13. Falchetto, R., Vorherr, T., Brunner, J., and Carafoli, E. (1991) *J. Biol. Chem.* **266,** 2930–2936
14. Falchetto, R., Vorherr, T., and Carafoli, E. (1992) *Protein Sci.* **1,** 1612–1621
15. Kim, E., DeMarco, S. J., Marfatia, S. M., Chishti, A. H., Sheng, M., and Strehler, E. E. (1998) *J. Biol. Chem.* **273,** 1591–1595
16. DeMarco, S. J., and Strehler, E. E. (2001) *J. Biol. Chem.* **276,** 21594–21600
17. Zabe, M., and Dean, W. L. (2001) *J. Biol. Chem.* **276,** 14704–14709
18. DeMarco, S. J., Chicka, M. C., and Strehler, E. E. (2002) *J. Biol. Chem.* **277,** 10506–10511
19. Schuh, K., Uldrijan, S., Telkamp, M., Röthlein, N., and Neyses, L. (2001) *J. Cell Biol.* **155,** 201–205
20. Schuh, K, Uldrijan, S, Gambaryan, S., Röthlein, N., and Neyses, L. (2003)

J. Biol. Chem. **278,** 9778–9783
21. Goellner, G. M., DeMarco, S. J., and Strehler, E. E. (2003) *Ann. N. Y. Acad. Sci.* **986,** 461–471
22. Dammann, R., Li, C., Yoon, J.-H., Chin, P. L., Bates, S., and Pfeifer, G. P. (2000) *Nat. Genet.* **25,** 315–319
23. Vos, M.D., Chad, A. E., Bell, A., Birrer, M. J., and Clark, G. J. (2000) *J. Biol. Chem.* **275,** 35669–35672
24. Sambrook, J., Fritsch, E. F., and Maniatis, T. (1989) *Molecular Cloning: A Laboratory Manual*, Cold Spring Harbor Laboratory Press, Cold Spring Harbor, NY
25. Sugden, P. H., and Clerk, A. (2000) *Trends Cardiovasc. Med.* **10,** 1–8
26. Hunter, J. J., Tanaka, N., Rockman, H. A., Ross, J., Jr., and Chien, K. R. (1995) *J. Biol. Chem.* **270,** 23173–23178
27. Shivakumar, L., Minna, J., Sakamaki, T., Pestell, R., and White, M. A. (2002) *Mol. Cell. Biol.* **22,** 4309–4318
28. Kim, S.-T., Lim, D.-S., Canman, C. E., and Kastan, M. B. (1999) *J. Biol. Chem.* **274,** 37538–37543
29. Force, T., and Bonventre, J. V. (1998) *Hypertension* **31,** 152–161
30. Liu, L., Tommasi, S., Lee, D.-H., Dammann, R., and Pfeifer, G. P. (2003) *Oncogene* **22,** 8125–8136
31. Rivas, F. V., O'Keefe, J. P., Alegre, M.-L., and Gajewski, T. F. (2004) *Mol. Cell. Biol.* **24,** 1628–1639
32. Schwab, B. L., Guerini, D., Didszun, C., Bano, D., Ferrando-May, E., Fava, E., Tam, J., Xu, D., Xanthoudakis, S., Nicholson, D. W., Carafoli, E., and Nicotera, P. (2002) *Cell Death Differ.* **9,** 818–831
33. Chami, M., Ferrari, D., Nicotera, P., Paterlini-Bréchot, P., and Rizzuto, R. (2003) *J. Biol. Chem.* **278,** 31745–31755
34. Sasamura, S., Furukawa, K.-I., Shiratori, M., Motomura, S., and Ohizumi, Y. (2002) *Jpn. J. Pharmacol.* **90,** 164–172
35. Cowan, K. J., and Storey, K. B. (2003) *J. Exp. Biol.* **206,** 1107–1115
36. Bertin, J., Wang, L., Guo, Y., Jacobson, M. D., Poyet, J.-L., Srinivasula, S. M., Merriam, S., DiStefano, P. S., and Alnemri, E. S. (2001) *J. Biol. Chem.* **276,** 11877–11882
37. Hofmann, K. (1999) *Cell Mol. Life Sci.* **55,** 1113–1128
38. Hammes, A., Oberdorf-Maass, S., Rother, T., Nething, K., Gollnick, F., Linz, K. W., Meyer, R., Hu, K., Han, H., Gaudron, P., Ertl, G., Hoffman, S., Ganten, U., Vetter, R., Schuh, K., Benkwitz, C., Zimmer, H. G., and Neyses, L. (1998) *Circ. Res.* **83,** 877–888
39. Fujimoto, T. (1993) *J. Cell Biol.* **120,** 1147–1157
40. Ko, Y.-G., Lee, J.-S., Kang, Y.-S., Ahn, J.-H., and Seo, J.-S. (1999) *J. Immunol.* **162,** 7217–7223
41. Oxhorn, B. C., and Buxton, I. L. O. (2003) *Cell. Signalling* **15,** 489–496
42. Paszty, K., Verma, A. K., Padanyi, R., Filoteo, A. G., Penniston, J. T., and Enyedi, A. (2002) *J. Biol. Chem.* **277,** 6822–6829
43. Tommasi, S., Dammann, R., Jin, S.-G., Zhang, X.-F., Avruch, J., and Pfeifer, G. P. (2002) *Oncogene* **21,** 2713–2720
44. Vos, M. D., Ellis, C. A., Elam, C., Ülkü, A. S., Taylor, B. J., and Clark, G. J. (2003) *J. Biol. Chem.* **278,** 28045–28051
45. Roy, S., Luetterforst, R., Harding, A., Apolloni, A., Etheridge, M., Stang, E., Rolls, B., Hancock, J. F., and Parton, R. G. (1999) *Nat. Cell Biol.* **1,** 98–105
46. Prior, I. A. (2003) *Biochemist* **25,** 22–24